

Line and Recombination Emission in the ASDEX Upgrade Divertor at High Density

B. Napióntek, U. Wenzel*, K. Behringer, D. Coster, J. Gafert, R. Schneider, A. Thoma, M. Weinlich and ASDEX Upgrade-Team

Max-Planck-Institut für Plasmaphysik, EURATOM Association, Garching and *Berlin

Introduction

The most promising divertor regime for ITER is the detached, high density divertor with its high radiation losses. Therefore we focus the spectroscopic investigations on this state to understand the emission properties, the behavior of the intrinsic impurity sources and the plasma parameters.

The radiation of carbon and deuterium was investigated by means of a scanning VUV spectrometer. The spatial distributions of the resonance line emission of carbon and deuterium were integrated to obtain the total radiation power losses. A small temperature dependent correction to get the total carbon radiation in the divertor was also included. The density dependence of the radiated power was measured in a density ramp with 3.5 MW heating power.

Detached divertor plasmas are characterized by strong hydrogen radiation which can be used for plasma diagnostics. By these means spectroscopical measurements of electron temperature and density in ASDEX Upgrade were carried out which are comparable to the recent experiments at Alcator C-Mod [1]. We will discuss the properties of cold, dense divertor plasmas and describe a method for T_e and n_e measurements which shall be compared with results of plasma modelling using the codes B2-EIRENE.

Despite the very low temperature in front of the plate carbon emission is high in the detached divertor. Therefore, we have studied the CD band in the visible to estimate the carbon influx via chemical erosion.

Experiment

Experimental investigations were carried out with two spectroscopic systems. The divertor spectrometer (s. fig. 1) observed the plasma along several sightlines in the poloidal cross-section. There are 30 sightlines viewing the plasma parallel to the outer target plate in a distance of 1...90 mm, another set of 16 sightlines is arranged fan-like. The collected light was fed via optical fibers to a Czerny-Turner or a Fastie-Ebert (Echelle grating) spectrometer with low and high spectral resolution, respectively. Several lines of sight were detected simultaneously by means of a fast CCD camera.

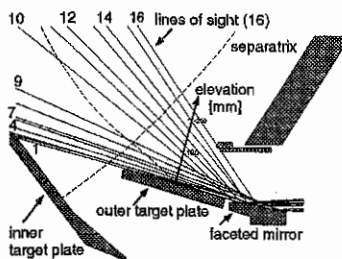


Figure 1: Arrangement of the 16 poloidal sightlines of the divertor spectrometer. Another set of 30 sightlines views the plasma parallel to the outer target plate.

The boundary layer spectrometer (s. fig. 2) scanned the whole poloidal cross-section. In this way the inner and outer target plate could be observed. The light was analyzed by two spectrometers in the VUV and visible spectral range.

Results: Power losses during a density ramp

The divertor radiation was investigated in an L-mode discharge with 3.5 MW heating power. By means of gas puffing, the line-averaged density in the midplane increased from $4.5 \cdot 10^{19} m^{-3}$ to $6.5 \cdot 10^{19} m^{-3}$. The ion saturation current of Langmuir probes in the target plates first increased, but then dropped by a factor of 4 at 3.1 s due to detachment. Spectroscopically, power losses were obtained by summing over the resonance lines of carbon and deuterium in the VUV spectral range. In Fig. 3 the results are compared to the bolometer measurements. The power losses rise with increasing midplane density. The ratio of the carbon to deuterium emission changes from 1:1 to 2:1 during the ramp. Main radiator is the CIII ion. The spectroscopically measured values lie 30% below the bolometer values, possibly caused by other impurities (O, F, Cl, B).

The highest radiated power is observed in the detached divertor despite the very low temperature of about 1 eV (s. next section), i.e. there is no drastic reduction of the carbon source. The high intensity of the CD band emission even at detachment suggests the process of chemical erosion. From the measured band intensity the methane influx can be calculated. On the other hand, the methane influx can be calculated using the ion flux to the target plates measured by Langmuir probes and the yield for chemical erosion. In Fig. 4 we compare both methods. The absolute values agree well in the attached phase. During detachment the influx calculated from the measured ion flux deviated significantly from the spectroscopic measurements. This is probably due to chemical erosion caused by the flux of atoms onto the target plates.

Results: Recombining plasma

At maximum radiation the divertor is already detached. As indicated by the location of the emission zones of CIII and CIV the thermal front position is close to the X-point and the major part of the divertor is cold.

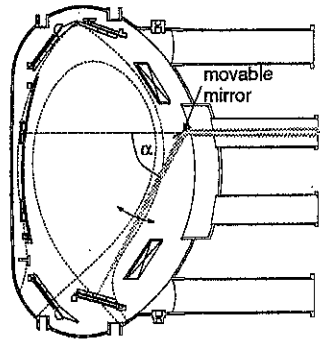


Figure 2: Schematic view of the boundary layer spectrometer. A movable mirror allows scanning of the whole poloidal cross-section.

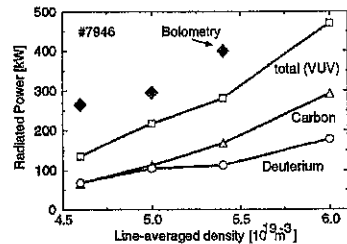


Figure 3: Power radiated in the outer divertor as a function of the midplane density: carbon, deuterium and sum of both; compared total and measured by bolometers.

Under these conditions we observed the Balmer and Paschen continuum radiation and line radiation of the Balmer series up to transitions from level $n = 14$. When the plasma detaches there is a drop in electron temperature and an increase in electron density and therefore strongly increased rates for radiative and three-body recombination (s. [2]). This leads to a strong increase in hydrogen radiation. Fig. 5 compares two spectra at different times in an L-mode density limit discharge similar to the one discussed above. The ratio of Balmer to Paschen continuum radiation provides a sensitive method to measure the electron temperature. During the detachment the electron temperature decreased to $0.8 \dots 1.4 \text{ eV}$ in the whole divertor. The electron density was determined from the absolutely calibrated Balmer continuum emission giving maximum values of $1 \cdot 10^{21} \text{ m}^{-3}$. From the spectrum shown in Fig. 5 $1.1 \cdot 10^{20} \text{ m}^{-3}$ was determined which is about a factor of 2 higher than the midplane density.

In order to investigate the optical thickness of the divertor plasma we measured simultaneously L_β and H_α with the boundary layer spectrometer. At moderate divertor densities the ratio of H_α to L_β intensities starts to increase with density indicating the effect of optical thickness. At higher densities and regarding L_α the effect must be even more pronounced. Thus in the region of high density plasmas, where the observed continuum radiation is preferentially emitted, recombination into the ground state via excited states is reduced. Therefore we expect that net recombination occurs in the outer zone of the divertor plasma and possibly near the target due to enhanced recombination rates by molecule encounters.

The arrays of lines of sight of the divertor spectrometer allow measurements of spatial T_e and n_e profiles. Spatial resolution is possible in the direction perpendicular to the target plates whereas along the line of sight the emission is integrated (s. Fig. 1). Due to dependence of the emissivity on n_e^2 the region with the highest density dominates the intensity. The temperature measurements represent the region with the highest temperature along the line of sight because of the steep dependence of the Balmer to Paschen

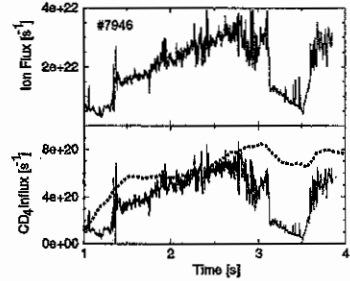


Figure 4: Comparison of the methane influx measured spectroscopically (dotted line) and calculated from the ion flux to the target plate measured by Langmuir probes which is given separately in the upper graph.

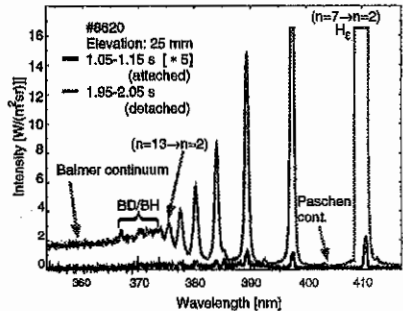


Figure 5: Spectra around the Balmer series limit measured with the divertor spectrometer. The midplane density rises from $4.1 \cdot 10^{19} \text{ m}^{-3}$ (at 1.1 s) to $6.7 \cdot 10^{19} \text{ m}^{-3}$ (at 2.0 s) leading to fully detachment. The marked regions of continuum radiation are used for temperature determination.

continuum ratio for $T_e \leq 2 \text{ eV}$. Therefore we get upper limits for T_e and n_e along the line of sight. This is illustrated in Fig. 6 which shows results of the modelling of the fully detached divertor plasma using B2-EIRENE [3] compared with the experiment.

Near the outer target plate (within about 10 mm) the modelled mean temperatures decrease due to the lower temperatures in the outer divertor. The spectroscopic temperature measurements are dominated by the inner divertor. Thus the measured spatial profiles can only be interpreted as profiles of mean values of T_e and n_e in the emission zone of the outer divertor at greater distances to the target plate. Therefore qualitative differences between the modelled mean parameters and the measurements (s. Fig. 6) especially for T_e near the target are to be expected. The agreement at greater distances to the target plates and for the electron density is quite good. We will overcome the problem of integrating along the outer and inner divertor in the new divertor configuration of ASDEX Upgrade where both parts of the divertor will be observed separately.

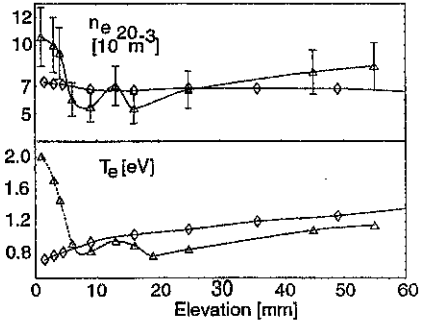


Figure 6: Modelling (\diamond) and measurements (Δ), #8620 at 2.7 s) of T_e and n_e profiles. The rise of measured electron temperature near the target plate is due to the effect of the inner divertor on line integrated intensity.

Summary

Fully detached divertor plasmas in ASDEX Upgrade are characterized by low temperatures $T_e < 2 \text{ eV}$, high density $n_e \lesssim 1 \cdot 10^{21} \text{ m}^{-3}$ and radiative and three-body recombination in the divertor volume. Despite the low electron temperature, carbon influx is very high caused by chemical erosion. The detached outer divertor reaches about 0.5 MW radiated power due to both the high influx and the high electron density. Main radiators are deuterium and CIII.

The ratio of Balmer to Paschen continuum radiation provides a sensitive method for temperature measurements, however, the line integrated values are strongly weighted by the highest temperatures along sightline. Spatial profiles of electron density and temperature are in good agreement with first results of modelling recombining divertor plasmas in ASDEX Upgrade with B2-EIRENE.

References

- [1] LUMMA, D. TERRY, J. L., and LIPSCHULTZ, B., PFC/JA-96-33, MIT, 1996
- [2] BORRAS, K., et al., this conference, P4.019
- [3] COSTER, D., et al., this conference, P4.013